Pergamon

Mechanics Research Communications, Vol. 27, No. 6, pp. 685–690, 2000

0093-6413/00/$–see front matter

PII: S0093-6413(00)00149-X

ON FICTITIOUS FREQUENCIES USING DUAL BEM FOR NON-UNIFORM RADIATION PROBLEMS OF A CYLINDER

J. T. Chen*, C. T. Chen**, K. H. Chen* and I. L. Chen*
* Department of Harbor and River Engineering, Taiwan Ocean University, Keelung, Taiwan
** Department of Oceanography, Taiwan Ocean University, Keelung, Taiwan

(Received 28 January 2000; accepted for print 5 October 2000)

Introduction

The fictitious frequencies, or so called irregular frequencies, have been studied by mathematicians [1, 2, 3, 4] and boundary element researchers [5, 6, 7, 8, 9, 10]. For the continuous system, Chen [11, 12] proved analytically using the dual series model that the positions where the fictitious frequencies occur depends on the integral representation for the solution. The types of boundary conditions can not change the positions once the integral formulation is chosen. Later, Chen [17] applied the theory of circulant to understand the occuring mechanism of irregular frequencies in a discrete system by considering a circular example. However, no numerical examples using the dual BEM were provided in the two papers [12, 17].

In this paper, a dual BEM program was developed to study the fictitious frequencies numerically. The positions of fictitious frequencies for the exterior problems using the UT (singular integral equation) or the LM (hypersingular integral equation) formulation are plotted. Two numerical examples of non-uniform radiation problems with the Dirichlet and Neumann boundary conditions, are illustrated to show the mechanism of fictitious frequencies. Numerical results using the dual BEM program are verified in comparision with the analytical solutions [19]. It is shown that the integral formulation, either singular or hypersingular equation, has different fictitious frequencies. However, the positions of irregular frequencies are independent of the types of the boundary conditions, once the method, either the UT or the LM method, is adopted. Based on the theoretical proof for a continuous system [12], for a discrete system using circulants [17] and the present numerical study using the dual BEM, some misleading statements for the positions of irregular values in the literatures can be clarified.

Dual integral formulation for a two-dimensional exterior acoustic radiation problem

The governing equation for an exterior acoustic problem is the Helmholtz equation as follows:

$$(\nabla^2 + k^2)u(x_1, x_2) = 0, \quad (x_1, x_2) \in D,$$

where ∇^2 is the Laplacian operator, D is the domain of the cavity and k is the wave number, which is angular frequency over the speed of sound. For simplicity, a radiation problem is considered only. The boundary conditions can be either the Neumann or Dirichlet type.

Based on the dual formulation, the dual equations for the boundary points are

$$\pi u(x) = C.P.V. \int_B T(s,x)u(s)dB(s) - R.P.V. \int_B U(s,x)t(s)dB(s), \quad x \in B \tag{1}$$

$$\pi t(x) = H.P.V. \int_B M(s,x)u(s)dB(s) - C.P.V. \int_B L(s,x)t(s)dB(s), \ x \in B \tag{2}$$

where *C.P.V.*, *R.P.V.* and *H.P.V.* denote the Cauchy principal value, the Riemann principal value and the Hadamard principal value, $t(s) = \frac{\partial u(s)}{\partial n_s}$, B denotes the boundary enclosing D and the explicit forms of the four kernels, U, T, L and M, can be found in [11, 14, 15].

Dual BEM formulation for a two-dimensional exterior acoustic radiation problem

The linear algebraic equations for an interior problem discretized from the dual boundary integral equations can be written as

$$[T^i_{pq}]\{u_q\} = [U^i_{pq}]\{t_q\} \tag{3}$$

$$[M^i_{pq}]\{u_q\} = [L^i_{pq}]\{t_q\}, \tag{4}$$

where the superscript "i" denotes the interior problem, $\{u_q\}$ and $\{t_q\}$ are the boundary potential and flux, and the subscripts p and q correspond to the labels of the collocation element and integration element, respectively. The influence coefficients of the four square matrices $[U], [T], [L]$ and $[M]$ can be represented as

$$U^i_{pq} = R.P.V. \int_{B_q} U(s_q, x_p)dB(s_q) \tag{5}$$

$$T^i_{pq} = -\pi\delta_{pq} + C.P.V. \int_{B_q} T(s_q, x_p)dB(s_q) \tag{6}$$

$$L^i_{pq} = \pi\delta_{pq} + C.P.V. \int_{B_q} L(s_q, x_p)dB(s_q) \tag{7}$$

$$M^i_{pq} = H.P.V. \int_{B_q} M(s_q, x_p)dB(s_q), \tag{8}$$

where B_q denotes the q^{th} element and $\delta_{pq} = 1$ if $p = q$; otherwise it is zero. The detail to determine the influence coefficients can be found in [15]. For the exterior problem, we have

$$[T^e_{pq}]\{u_q\} = [U^e_{pq}]\{t_q\} \tag{9}$$

$$[M^e_{pq}]\{u_q\} = [L^e_{pq}]\{t_q\}. \tag{10}$$

where the superscript "e" denotes the exterior problem. According to the dependence of the outnormal vectors in these four kernel functions for the interior and exterior problems, their relationship can be easily found as shown below [16]:

$$U^i_{pq} = U^e_{pq} \tag{11}$$

$$M^i_{pq} = M^e_{pq} \tag{12}$$

$$T^i_{pq} = \begin{cases} -T^e_{pq}, & if \ p \neq q, \\ T^e_{pq}, & if \ p = q \end{cases} \tag{13}$$

$$L^i_{pq} = \begin{cases} -L^e_{pq}, & if\ p \neq q, \\ L^e_{pq}, & if\ p = q. \end{cases} \tag{14}$$

Based on the relations in Eqs.(11) $\sim$ (14), the dual BEM program can be easily extended to solve for exterior problems.

In order to avoid the problem of fictitious frequency, the Burton and Miller formulation [1] is employed by considering the following equation,

$$\{[T^e_{pq}] + \frac{i}{k}[M^e_{pq}]\}\{u_q\} = \{[U^e_{pq}] + \frac{i}{k}[L^e_{pq}]\}\{t_q\} \tag{15}$$

where $i^2 = -1$.

Numerical examples

For the first example, a non-uniform radiation problem from a sector of a cylinder [19] is considered. The model has a constant inhomogeneous value on an arc $(-\alpha < \theta < \alpha)$ and vanishing elsewhere. Two points of potential discontinuity in the boundary data can be found. The governing equation and boundary condition are shown in Fig.1. The normalized analytical solution to this cylinder problem of a radius a is

$$u(r,\theta) = \frac{2}{\pi}\sum_{n=0}^{\infty}{}' \frac{sin(n\alpha)}{n}\frac{H^{(1)}_n(kr)}{H^{(1)}_n(ka)}cos(n\theta), \tag{16}$$

where $H^{(1)}_n(kr)$ is the Hankel function of the first kind of order n, and the symbol $'$ denotes that the first term $(n = 0)$ is halved. We select $\alpha = 20^o$. Fig.2 shows the contour plot for the real part of the analytical and numerical solutions. The analytical solution is obtained by using 20 terms series representations. Sixty-three elements are adopted in the dual BEM mesh. The positions where the irregular values occur can be found in Fig.3 for the solution $t(a,0)$ versus k by using either the UT or the LM equation only. It is found that irregular values occur at J^m_n, the zeros of the Bessel function of the first kind of order n, $J_n(ka)$, for the UT formulation, while LM formulation has the irregular values of J'^m_n, the zeros of the derivative of the Bessel function of the first kind of order n, $J'_n(ka) = 0$. The zeros for the Bessel functions and their derivatives are shown in Table 1. Also, the Burton and Miller formulation can avoid the numerical resonace and the UT and LM results agree well except at the irregular wave numbers as shown in Fig.3. The UT method is found to be superior to LM method since the participation factor [17] for the fictitious modes is lower. The performance of the dual BEM in comparison with the analytical solution and the DtN results [19] is quite good. Also, the analytical solution is shown in Fig.3 by methods of accelerating convergence [18] although the series solution is oscillating.

In order to clarify how the irregular frequencies depend on the types of boundary conditions, the second example with the Neumann boundary condition is designed in Fig.4. The analytical solution is

$$u(r,\theta) = \frac{2}{\pi}\sum_{n=0}^{\infty}{}' \frac{-1}{k}\frac{sin(n\alpha)}{n}\frac{H^{(1)}_n(kr)}{H^{(1)\prime}_n(ka)}cos(n\theta). \tag{17}$$

where $H_n^{(1)\prime}(ka)$ denotes the derivative of the Hankel function of the first kind of order n. The contour plot for the real-part solution is shown in Fig.5. It indicates that numerical results agree well with the analytical solution. Also, it is interesting to find that the irregular frequencies in Fig.6 occurs at the same positions in comparison with those of Fig.3. The UT method agrees better than LM method since the participation factor [17] for the fictitious modes is lower. This confirms the conclusion in [12, 17] that the irregular frequencies depend on the integral formulation (UT or LM method) instead of the types of boundary conditions (Dirichelet or Neumann).

Concluding remarks

The mechanism why fictitious frequencies occur in the dual BEM has been examined by considering non-uniform radiation problems of a cylinder. It is found that the irregular values depend on the integral formulation, the UT or the LM equation, instead of the types of boundary condition. The examples show that the first UT equation results in fictitious frequencies at the zeros of $J_n(ka) = 0$, which are associated with the interior acoustic frequencies of essential homogeneous boundary conditions, while the second LM equation produces fictitious frequencies at the zeros of $J_n'(ka) = 0$, which are associated with the interior eigenfrequency of natural homogeneous boundary conditions. The numerical results using the dual BEM program agree very well with the analytical solutions.

References

[1] Burton, A. J. and Miller, G. F., Proc. R. Soc. London Ser. A, 323, 201(1971).

[2] Schneck, H. A., J. Acoust. Soc. Amer. 44(1), 41(1968).

[3] Martin, P. A., Q. Jl. Mech., 27, 386(1980)

[4] Kleinman, R. E. and Roach, G. F., SIAM Rev., 16, 214(1974).

[5] Shaw, R. P., Boundary Integral Equation Methods Applied to Wave Problems, Chapter 6, in Developments in Boundary Element Methods, Vol.2, edited by P. K. Banerjee and R. P. Shaw, 121(1979).

[6] Rezayat, M., Shippy, D. J. and Rizzo, F. J., Comp. Meth. Appl. Mech. Engng., 55, 349(1986).

[7] Rizzo, F. J., Shippy, D. J. and Rezayat, M., Final Project Report for NSF Research Grant CEE-8013461(1985).

[8] Huang, I. T. and Fan, C. N., in Proceedings of the Institute of Mechanical Engineers, IMech Publ.(1991).

[9] SYSNOISE Manual, Numerical Institute of Technology (1992).

[10] Chen, J. T.,Chen, I. L. and Liang, M. T., On irregular frequencies in wave radiation solutions using dual boundary element method, ISOPE 99 Conference, 260-265, Brest, France (1999).

[11] Chen, J. T. and H.-K. Hong, Boundary Element Method, New World Press (1992). (in Chinese)

[12] Chen, J. T., Mech. Res. Comm., 25, 529(1998).

[13] Chen, J. T. and Kuo, S. R., Mech. Res. Comm., 27, 1(2000).

[14] Chen, J. T. and Hong, H.-K., ASME, Appl. Mech. Rev., 52, 17(1999).

[15] Chen, J. T. and Chen, K. H., Engng. Anal. Bound. Elem., 21, 105(1998).

[16] Chen, J. T., Liang, M. T. and Yang, S. S., Engng. Anal. Bound. Elem., 16, 333(1995).

[17] Chen, C. T., Master thesis, Department of Oceanography, National Taiwan Ocean University, 2000.

[18] Chen, J. T. Chen, Hong, H.-K., Yeh, C. S. and Chyuan, S. W., Earthq. Engng. Struct. Dyn., 25, 909(1996).

[19] Harari, I. P., Barbone, E., Slavutin, M. and Shalom, R., Int. J. Numer. Meth. Engng., 41, 1105(1998).

Table 1 Zeros of the Bessel functions for $J_n(k)$ and $J'_n(k)$

J_n^m	$m=1$	$m=2$	$m=3$	$m=4$	$m=5$
$J_0(k)=0, n=0$	2.4048	5.5201	8.6537	11.7915	14.9309
$J_1(k)=0, n=1$	3.8317	7.0156	10.1735	13.3237	16.4706
$J_2(k)=0, n=2$	5.1356	8.4172	11.6198	14.7960	17.9598
$J_3(k)=0, n=3$	6.38016	9.76102	13.0152	16.22346	19.40941
$J_4(k)=0, n=4$	7.58834	11.0647	14.3725	17.6160	20.8269
$J_5(k)=0, n=5$	8.77148	12.3386	15.7002	18.9801	22.2178
$J_n'^m$	$m=1$	$m=2$	$m=3$	$m=4$	$m=5$
$J'_0(k)=0, n=0$	0	3.83171	7.01559	10.17346	13.3237
$J'_1(k)=0, n=1$	1.84118	5.33144	8.53632	11.70600	14.8636
$J'_2(k)=0, n=2$	3.05424	6.70713	9.96947	13.17037	16.3475
$J'_3(k)=0, n=3$	4.20119	8.01524	11.3459	14.5858	17.7887
$J'_4(k)=0, n=4$	5.31755	9.2824	12.6819	15.9641	19.1960
$J'_5(k)=0, n=5$	6.41562	10.5199	13.9872	17.3128	20.5755

J_n^m and $J_n'^m$ are the mth zeros of the Bessel functions, $J_n(k)$ and $J'_n(k)$, respectively.

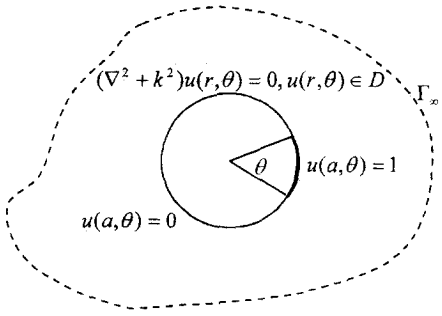

Fig 1. The nonuniform radiation problem (Dirichlet type) for a cylinder.

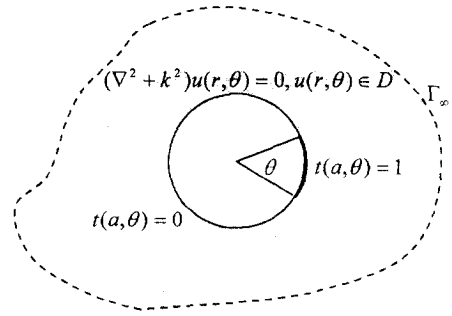

Fig 4. The nonuniform radiation problem (Neumann type) for a cylinder.

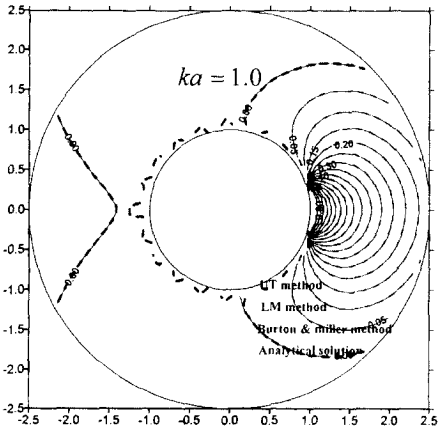

Fig 2. The contour plot for the real-part solutions (analytical solution: dashed line, numerical result: solid line).

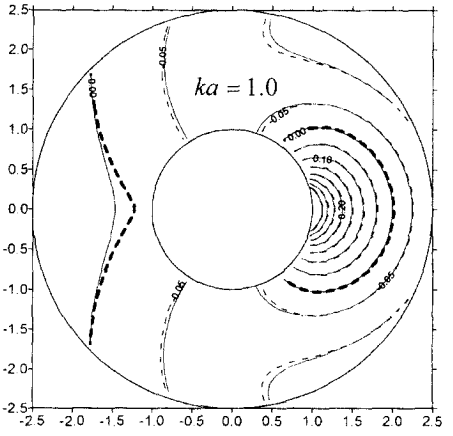

Fig 5. The contour plot for the real-part solutions (analytical solution: dashed line, numerical result: solid line).

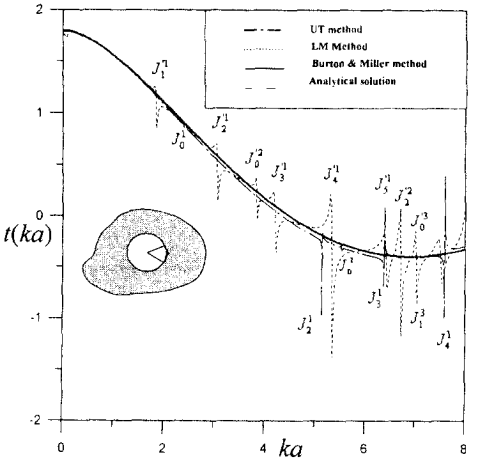

Fig3. The positions of irregular values using different methods.

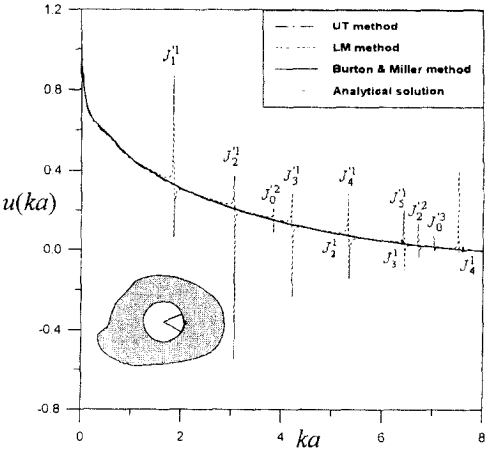

Fig6. The positions of irregular values using different methods.